

The Characteristic Analysis of a Nano Positioning Actuator

Jong-Seok Rho and Hyun-Kyo Jung
 School of Electrical Engineering
 Seoul National University University
 San 56-1, Sillim-dong, Gwanak-gu, Seoul, 151-742
 Korea
<http://elecmech.snu.ac.kr/>

Abstract: - In this paper, we report on our study of a Nano Positioning Actuator (NPA), which uses an impact/inchworm mechanism. Many kinds of similar precise positioning actuators, which use the same working mechanism, are being and have been proposed by many researchers for several decades. But, a characteristic analysis and design method for the NPA has not been proposed yet. Also, the characteristic analysis and design methods of similar machines were only approximate and ineffective. This was because they used only a rough analytic method or an experimental trial and error method for analysis and design. Although, some papers proposed analytic equations for the characteristic analysis, they did not clearly elucidate the complicated working mechanisms. They did not take all effective components and workings into consideration such as the slip phenomenon, the electromagnetic force relation, the frequency dependency, and so on.

Hence, we present in this paper an analysis methodology for the NPA using the 3D FEM combined with an analytic method, shedding light on the complex working mechanism, and taking all effective components into consideration for an exact and effective characteristic analysis of the NPA and similar machines. In this study, the mechanical system and the electrical control system of an NPA were prototyped. Finally, the effectiveness of an NPA considering such aspects as size, cost, and so on was validated by experiment. Also, the reasonableness of a clarified complex working mechanism taking all effective components into account was verified by experimental data.

Key-Words: - Actuator, finite element method, impact mechanism, inchworm mechanism, nano, piezoelectric, manipulator

1 Introduction

Important trends in industry are miniaturization and precision. These trends in turn drive the increasing demand for precise positioning actuators. As a consequence, many precise positioning actuators are being and have been proposed by many researchers for several decades. But, most of these actuators need very complex designs, high precision manufacturing, error compensators, temperature controls, and so on. Hence, most of the existing precise positioning actuators have problems. These problems include their large sizes, their large consumption of energy, and their large production and maintenance costs [1]-[18]. To address these problems, many kinds of precise positioning actuators, which use the impact or inchworm mechanism, have been proposed by many researchers [1]-[18]. These machines have merits of being small in size, having low energy consumption, and being very economical in their production and maintenance costs. Therefore, the NPA, which uses an

impact/inchworm mechanism, was selected to study as the precise positioning actuator in our research.

There are many kinds of other precision machines, which use the same impact or inchworm mechanism as the NPA. References [1]-[18] discuss such machines. But, the characteristic analysis and design method of the NPA has not proposed yet. Also, the characteristic analysis and design methods of similar machines were approximate and ineffective. This is because they used only a rough analytic method or an experimental trial and error method for analysis and design. These methods did not clearly articulate the complex working mechanism taking all effective components into consideration. Some effective components and workings not taken into consideration are the slip phenomenon, the electromagnetic force relation, the frequency dependency, and so on. References [8] and [9] suggest the characteristics analysis method of machines which use the impact/inchworm mechanism by using an approximate analytic method. However, only a rough

characteristic analysis has been possible because rough analytic equations have been only used for the characteristic analysis without consideration of the complex working mechanism and all the effective components. In one example, reference [9] mentions the need for clarifying the relationship between the electromagnetic force and slippage, but this remains as an unsolved problem. To solve this problem and to exactly and effectively analyze the characteristic of machines which use the impact or inchworm mechanism, we suggest this analysis methodology for the NPA. We use a 3D FEM combined with an analytic method. This methodology shed light on the complex working mechanism and considers all effective components. These components include the slip phenomenon, the electromagnetic force relation, the frequency dependency, unbalanced shape, and so on.

In this research, the mechanical system and the electrical control system of an NPA were prototyped. Finally, the effectiveness of an NPA in the aspect of size, cost, and so on, the reasonableness of the clarified complex working mechanism taking all effective components into consideration, and the adequacy of the proposed analysis method were validated by comparing their outcomes with experimental data.

2 The Working Principle of the NPA

Fig.1 shows the construction of the NPA. Two electromagnets (EMs) and a piezoelectric ceramic constitute the NPA.

The simplified working principle is indicated in Fig.2 and Fig3. Fig. 3 is drawn only to simply explain the ideal step motion of the impact/inchworm mechanism. As shown in Fig. 3, the NPA moves to the right side by synchronizing three electrical input sources as indicated in Fig.2. The NPA can move to the left side by exchanging the left and right coil's electrical input source sequence with each other.

The working principle of the NPA is based on the inchworm principle and the impact mechanism. This means the NPA slides by the synchronous sequence of the attaching action and the cyclic elasticity motion. The synchronous sequence of attaching by the EM and expanding and contracting by the piezoelectric ceramic is the inchworm principle. The sliding by the expansion and the contraction of the piezoelectric ceramic is the impact mechanism [1]-[16].

In the real case, the inchworm/impact working mechanism is more complicated than the ideal mechanism which is shown in Fig. 3. This is because the slip phenomenon occurs as a result of the force difference in the system. In addition to the slip phenomenon, there is another condition that makes the working mechanism complicated. This condition is the different displacement of the forward-electromagnet (FW-EM) and the backward-electromagnet (BW-EM) if the system of an NPA is an unbalanced shape or material. Also, if the operating frequency is changed or if the system's material or shape is changed, then the displacement is changed. There are many other components that make the working mechanism complicated. The real step motion is represented in Fig.4. This motion is different from the ideal one as shown in Fig. 3. However, only the ideal step motion has been taken into consideration, although the real step motion is different from the ideal step motion, as shown in Fig. 3 and Fig.4. Hence, we suggest the analysis methodology of the NPA using a 3D FEM combined with an analytic method shedding light on the complex working mechanism and considering all effective components.

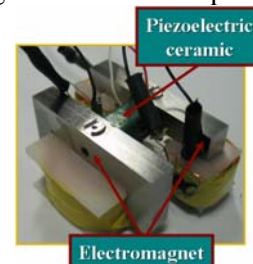


Fig.1. Prototyped NPA.

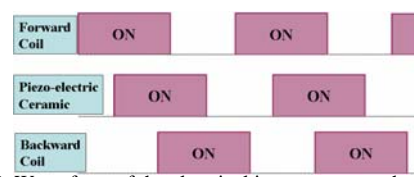


Fig.2. Wave form of the electrical input source to the NPA.

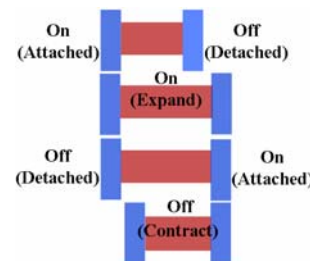


Fig.3. Step motion of the NPA according to the electrical input source of Fig.2.

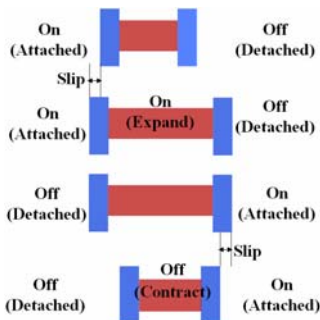


Fig.4. Real step motion of the NPA according to the electrical input source of Fig.2.

3 Prototype of the NPA

Fig.5 shows the prototype of an NPA. The important point here is that we suggest a three contact mechanism for an NPA to reduce the manufacturing cost and to guarantee the mechanical stability of the NPA. Fig.6 shows the flow chart of the control system for an NPA. As shown in Fig.6, we control the NPA by image control method using a microscope, a CCD camera, and a capture board. Fig.7 shows the flow chart of the driving circuit for an NPA. Three electrical input square waves with 90 degree phase difference are needed to operate an NPA, as shown in Fig.2. Therefore, the L297 chip, which is commonly used for a step motor driving circuit, is used for the generation of three electrical square waves with a 90 degree phase difference. Two waves, which have 180 degree phase difference, are used for the input source of the EMs. These two waves are amplified by the L298N chip. The third wave is used for the operation of the piezoelectric ceramic with high voltage. Therefore, a half-bridge circuit with a transistor is employed to amplify the voltage. Fig.8 shows the prototyped NPA's whole system.

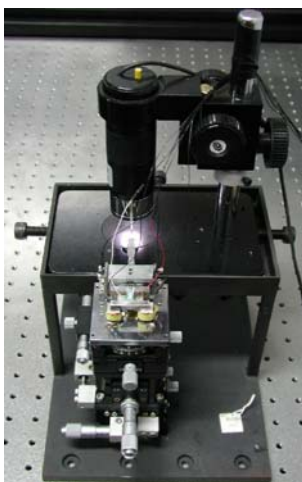


Fig.5. Prototyped mechanical system of a NPA.

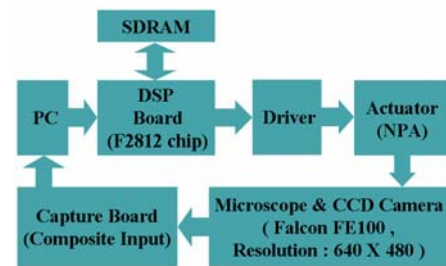


Fig.6. Flow chart of the control system for an NPA.

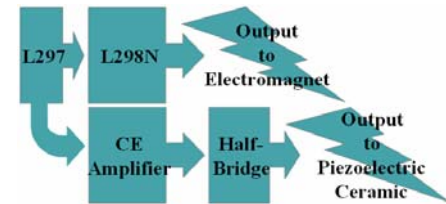


Fig.7. Flow chart of the driving circuit for an NPA.

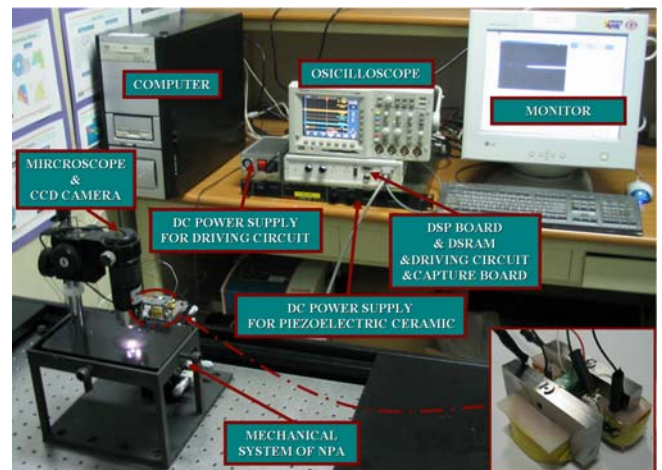


Fig.8. Prototyped NPA's whole system.

4 Characteristic Analysis and Experimental Results for the NPA

As briefly mentioned in II, the real step motion of an NPA follows the Fig. 4. This representation is more complicated than the ideal representation which is shown in Fig. 3. There are many effective components that make the working mechanism complicated in the real case, such as the slip phenomenon, the electromagnetic force relation, the frequency dependency, the unbalanced shape, and so on. But, only very approximate analytic methods or experimental trial and error methods have been used for the analysis and design of machines similar to the NPA. Only an ideal step motion has been used not taking the real step motion into consideration, until now. Therefore, the exact and efficient analysis and design has been impossible until now. Most of all, although the approximate analysis method of similar

machines to the NPA has been suggested, the analysis and design method of the NPA has not been proposed, yet. Therefore, we propose the analysis methodology of the NPA taking all effective components into consideration using 3D FEM combined with analytic method.

In this research, some effective components, such as the slip phenomenon and the electromagnetic force relationship of an NPA are defined as *external effective components* and some components, such as the NPA system's shape, material, operating frequency, input voltage, and so on are defined as *internal effective components* of this system.

4.1 The calculation of the ideal displacement at each EM Subsection

The first stage for the simulation of an NPA is the calculation of an *ideal displacement* by using a transient analysis with the 3D FEM. This analysis routine does not take *external effective components* into consideration such as the slip phenomenon and EM forces. It takes the internal system, itself, into consideration such as the NPA system's shape, material, operating frequency, input voltage, and so on. Hence, the simulated displacement, which is calculated by not taking the *external effective components* into consideration but only by taking the *internal effective components* into consideration, is called the *ideal displacement*. If the system is an unbalanced shape or material then each *ideal displacement* of a FW-EM and a BW-EM is different. If the operating frequency or the input voltages are changed then each *ideal displacement* of the FW-EM and the BW-EM is also changed.

Fig.9 shows the transient analysis result, by using the 3D FEM, of the NPA when a 50[V]/50[Hz] electrical source is applied to the piezoelectric ceramic. This analysis stage does not take the *external effective components* into consideration but only takes the *internal effective components* into consideration. Hence, the simulated displacement in Fig.9 is called the *ideal displacement* of an NPA. From this simulation routine, the *ideal displacements* of a FW-EM and a BW-EM are calculated.

The value of the calculated *ideal displacement* at the steady state of the FW-EM, $(u_F)_{ideal}$ is 829 [nm] and of the BW-EM, $(u_B)_{ideal}$ is -1000 [nm]. The FW-EM and the BW-EM are displaced asymmetrically because the shape of an NPA is asymmetric. Finally, the *ideal displacement* at each of a FW-EM and a BW-EM is

calculated by transient analysis using the 3D FEM and only taking *internal effective components* into consideration.

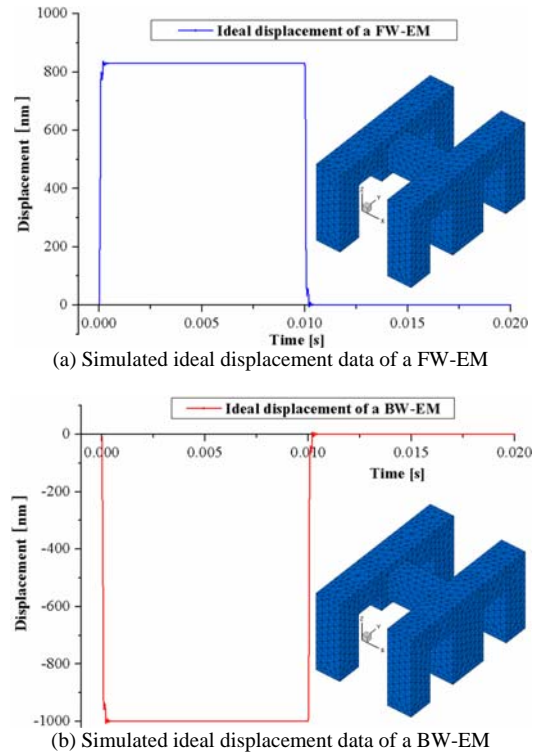


Fig.9. Simulated ideal displacement data of a NPA by 3D FEM, when 50[V]/50[Hz] electrical source is applied to piezoelectric ceramic.

4.2 The calculation of the total displacement at each EM

The second stage for the simulation of an NPA is the calculation of a mechanical displacement of an NPA by using an analytic method taking *external effective components*, such as slip losses and EM forces, into account. In our research, the NPA has been examined closely taking the complex working mechanism into consideration to calculate the *total displacement* of the NPA. The simulated final mechanical displacement, which is calculated by combining the *external effective components* and the *ideal displacement* result, is called the *total displacement* in this paper. Fig.10 shows the diagram of the mechanical displacement relation in the NPA combining the *ideal displacement* and *external effective components*.

From Fig. 10 and from the *Equation of Motion*, which explains the force and displacement relations [29],[30], we propose (45)-(58) for the calculation of the *total displacement* at each of the FW-EM and the BW-EM by closely taking the complex working mechanism

into consideration. The mechanical *total displacement* to the horizontal direction at each of the FW-EM, $(u_F)_{tot}$ and BW-EM, $(u_B)_{tot}$ can be expressed by (45)-(58) from Fig.10 and the *Equation of Motion*. When a piezoelectric ceramic expands, the *total displacement* can be defined by (45) and (46) ; when it contracts, by (47) and (48).

$$(u_F)_{tot} = +(u_F)_{ideal} - (u_F)_{t,r} + (u_B)_{t,r} \quad (45)$$

$$(u_B)_{tot} = -(u_B)_{ideal} + (u_B)_{t,r} - (u_F)_{t,r} \quad (46)$$

$$(u_F)_{tot} = -(u_F)_{ideal} + (u_F)_{t,r} - (u_B)_{t,r} \quad (47)$$

$$(u_B)_{tot} = +(u_B)_{ideal} - (u_B)_{t,r} + (u_F)_{t,r} \quad (48)$$

where,

$(u_F)_{t,r}$: the mechanical displacement of the FW-EM because of the total resisting horizontal force at the FW-EM

$(u_B)_{t,r}$: the mechanical displacement of the BW-EM because of the total resisting horizontal force at the BW-EM.

A mechanical displacement of the FW-EM because of the total resisting horizontal force at the FW-EM, $(u_F)_{t,r}$ can be expressed by :

$$\begin{aligned} (u_F)_{t,r} &= (u_F)_{ideal} \times \frac{(F_F)_{t,r}}{(F_F)_{eff.g}} \\ &= (u_F)_{ideal} \times \frac{(F_F)_{r,e} + (F_F)_{r,r,e} + (F_F)_{r,r}}{(m_F)_{eff} \times (a_F)_{eff}} \end{aligned} \quad (49)$$

where,

$$(m_F)_{eff} = m_F + \frac{m_p}{2} \quad (50)$$

and where,

$(F_F)_{t,r}$: the total resisting horizontal force at the FW-EM

$(F_F)_{eff.g}$: the effective value of the generated horizontal force at the FW-EM

$(F_F)_{r,e}$: the resisting horizontal force at the FW-EM due to the EM force of a FW-EM

$(F_F)_{r,r,e}$: the resisting horizontal force at the FW-EM due to the residual EM force at a FW-EM

$(F_F)_{r,r}$: the resisting horizontal force at the FW-EM due to rest forces at a FW-EM

$(m_F)_{eff}$: the effective mass of the FW-EM

$(a_F)_{eff}$: the effective acceleration of the FW-EM

m_F : the mass of the FW-EM

m_p : the mass of the piezoelectric ceramic.

A mechanical displacement of the BW-EM because of the total resisting horizontal force at the BW-EM, $(u_B)_{t,r}$ is derived by :

$$\begin{aligned} (u_B)_{t,r} &= (u_B)_{ideal} \times \frac{(F_B)_{t,r}}{(F_B)_{eff.g}} \\ &= (u_B)_{ideal} \times \frac{(F_B)_{r,e} + (F_B)_{r,r,e} + (F_B)_{r,r}}{(m_B)_{eff} \times (a_B)_{eff}} \end{aligned} \quad (51)$$

where,

$$(m_B)_e = m_B + \frac{m_p}{2} \quad (52)$$

and where,

$(F_B)_{t,r}$: the total resisting horizontal force at the BW-EM

$(F_B)_{eff.g}$: the effective value of the generated horizontal force at the BW-EM

$(F_B)_{r,e}$: the resisting horizontal force at the BW-EM due to the EM force of a BW-EM

$(F_B)_{r,r,e}$: the resisting horizontal force at the BW-EM due to the residual EM force at a BW-EM

$(F_B)_{r,r}$: the resisting horizontal force at the BW-EM due to rest forces at a BW-EM

$(m_B)_{eff}$: the effective mass of the BW-EM

$(a_B)_{eff}$: the effective acceleration of the BW-EM.

m_B : the mass of the BW-EM.

The ideal displacements, $(u_F)_{ideal}$ and $(u_B)_{ideal}$, are calculated by a 3D FEM as shown in Fig.9. Also, the effective value of generated horizontal forces, $(F_F)_{eff.g}$ and $(F_B)_{eff.g}$, are calculated by a 3D FEM and (49)-(52). The results are shown in Fig.11. In this study, these variables are constants. This is because the input electrical source to a piezoelectric ceramic is fixed only to be 50[V]/50[Hz]. The effective masses, $(m_F)_{eff}$ and $(m_B)_{eff}$ are also stationary. This is because the mass is not changed during the operation. The resisting horizontal forces which results from the rest forces at a FW-EM, $(F_F)_{r,r}$, is also a fixed variable equal to 0.01 [N]. This is because the resistance of a LM guide's

seal is the rest force in this research. The resisting horizontal forces which is results from the rest forces at a FW-EM, $(F_F)_{r,r}$, is a constant equal to 0 [N]. This is because there are no rest forces. Those fixed variables are tabulated in TABLE I where the sign follows the arrow directions of Fig.10.

Resisting horizontal forces due to the EM force, $(F_F)_{r,e}$ and $(F_B)_{r,e}$, are calculated by (53)-(54) and a 3D FEM. The resisting horizontal force due to the residual EM force at a FW-EM, $(F_F)_{r,r,e}$, and at a BW-EM, $(F_B)_{r,r,e}$ are calculated by (55) and (56). The simulation results are tabulated in TABLE II .

$$(F_F)_{r,e} = \mu_s \times (F_F)_{n,e} \tag{53}$$

$$(F_B)_{r,e} = \mu_s \times (F_B)_{n,e} \tag{54}$$

$$(F_F)_{r,r,e} = \mu_s \times (F_F)_{n,r,e} \tag{55}$$

$$(F_B)_{r,r,e} = \mu_s \times (F_B)_{n,r,e} \tag{56}$$

where,

- μ_s : the static frictional coefficient (0.17)
- $(F_F)_{n,e}, (F_B)_{n,e}$: the normal EM forces at the FW-EM and at the BW-EM
- $(F_F)_{n,r,e}, (F_B)_{n,r,e}$: the normal residual EM forces at the FW-EM and at the BW-EM

The simulated results of mechanical displacements to the horizontal direction are tabulated in TABLE III with the varying input electrical source to an EM. The sign of the listed values follows the arrow directions of Fig. 10.

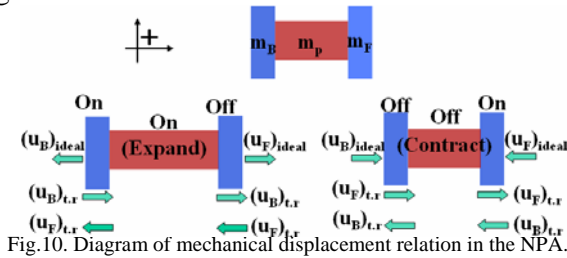
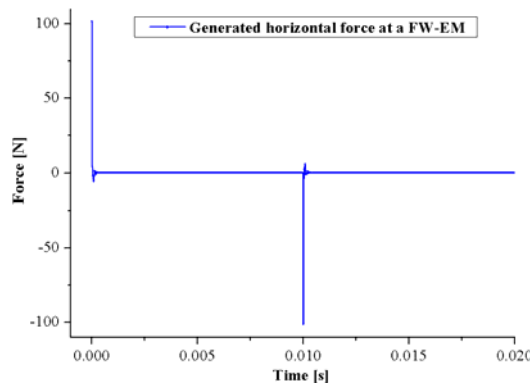
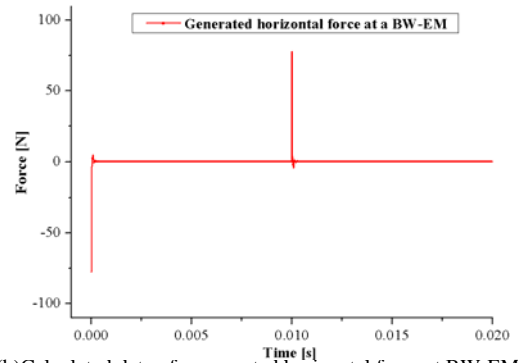


Fig.10. Diagram of mechanical displacement relation in the NPA.



(a) Calculated data of a generated horizontal force at FW-EM



(b) Calculated data of a generated horizontal force at BW-EM

Fig.11. Calculated results of a generated horizontal force.

4.3 The calculation of one cycle displacement at each EM

By applying (49)-(56) to (45)-(48), the *total displacement* to the horizontal direction of the FW-EM, $(u_F)_{tot}$ and BW-EM, $(u_B)_{tot}$ can be calculated about one cycle taking all *effective components* into consideration. The *total displacement* about one cycle has the same meaning as the resolution of an NPA. Hence, we propose (57) and (58) for the calculation of one cycle mechanical *total displacement* of the FW-EM, $(u_F)_{one_cyc}$ and the BW-EM, $(u_B)_{one_cyc}$. From these results, the resolution of an NPA can be simulated.

$$(u_F)_{one_cyc} = (u_F)_{tot_exp} + (u_F)_{tot_con} \tag{57}$$

$$(u_B)_{one_cyc} = (u_B)_{tot_exp} + (u_B)_{tot_con} \tag{58}$$

where,

$(u_F)_{tot_exp}$: the total displacement to the horizontal direction of the FW-EM when the piezoelectric ceramic expands

$(u_F)_{tot_con}$: the total displacement to the horizontal direction of the FW-EM when the piezoelectric ceramic contracts

$(u_B)_{tot_exp}$: the total displacement to the horizontal direction of the BW-EM, when the piezoelectric ceramic expands

$(u_B)_{tot_con}$: the total displacement to the horizontal direction of the BW-EM, when the piezoelectric ceramic contracts.

Finally, the mechanical one cycle displacement, in other words the resolution, of an NPA is calculated by

using (57) and (58) and TABLE II - TABLE III. The simulated data and the experimental data of the one cycle *total displacement* are shown in Fig. 12 and TABLE IV with varying the input electrical source of the EM. The result of the simulation, which has been calculated by the proposed method, fitted with the experimental data. This proved that the explained complex working mechanism, which is the impact and inchworm, taking the *internal* and the *external effective components* into account is correct and the proposed analysis methodology is reasonable. Therefore, it can be applicable to many other kinds of actuators which use the similar working mechanisms.

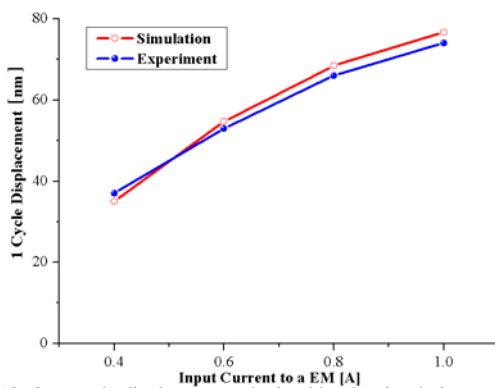


Fig.12. One cycle displacement obtained by the simulation and the experiment, according to the varying input current to the EM.

4.4 The application of the NPA for a specimen manipulator

In this research, we suggested the NPA for a specimen manipulator. Therefore, we set up the NPA's control mode for two types. One is the manual-mode and the other is the auto-mode. The manual mode is just controlling the NPA's needle manually. The auto-mode is controlling the NPA's needle automatically to manipulate specimen by setting a start-line, a mid-line, and an end-line and by determining the frequency values at each section, as shown in Fig.13-Fig.17. Fig.13-Fig.15 show when the forward-mode (FWM) and Fig.16 and Fig.17 show when the backward-mode (BWM) of an NPA.

In case of a FWM, the fast speed is needed when a needle approaches to a specimen. Therefore a user sets a start-line and a mid-line as shown in Fig.13. Then a user enters a high frequency value for the fast FW speed of a needle at this section. When a needle pricks a specimen, a slow speed is needed to avoid breakage of a specimen. Therefore, a user sets an end-line, as shown in Fig.13. The user enters a low frequency

value for the slow FW speed of the needle at this section. In the FWM, there are two speed change methods. One is the direct change of a speed by changing the frequency directly as shown in Fig.14. The other one is the gradual change of speed by changing the frequency gradually as shown in Fig.15. In the case of a BWM, the slow speed is needed until the time before a needle gets out of a specimen to avoid the breakage of a specimen. Therefore a user sets a start-line and a mid-line as shown in Fig.16. Then a user enters a low frequency value for the slow BW speed of the needle at this section. After the needle gets out of a specimen, the fast speed is needed. Therefore, a user sets an end-line, as shown in Fig.16. And a user enters a high frequency value for the fast BW speed of the needle at this section. In the BWM, the speed is changed directly by changing the frequency directly as shown in Fig.17.

From the experimental results, as shown in Fig.13-Fig.17, we validated that the proposed NPA is possible to use for a specimen manipulator.



Fig.13. Auto-control mode of a NPA for the use of a cell manipulator, in case of FWM.

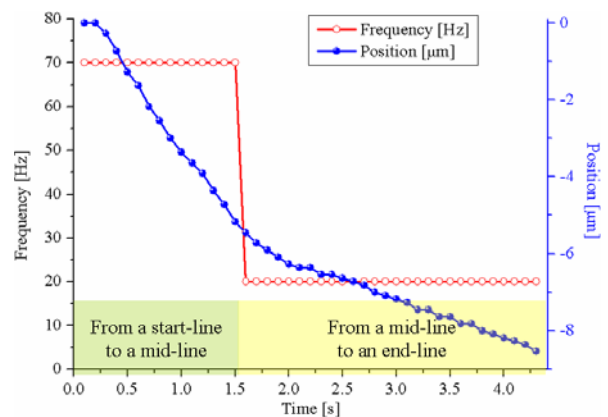


Fig.14. Experimental data of Fig.13, in case of the direct change of speed.

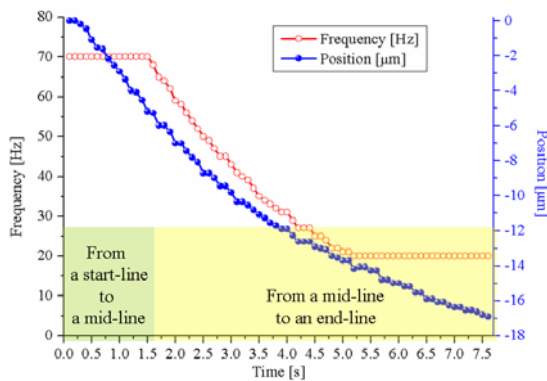


Fig.15. Experimental data of Fig.13, in case of the gradual change of speed.

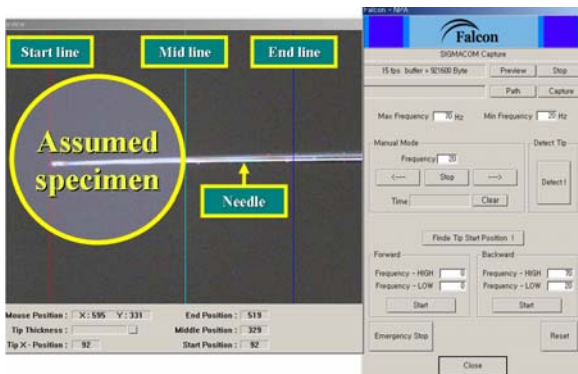


Fig.16. Auto-control mode of a NPA for the use of a cell manipulator, in case of BWM.

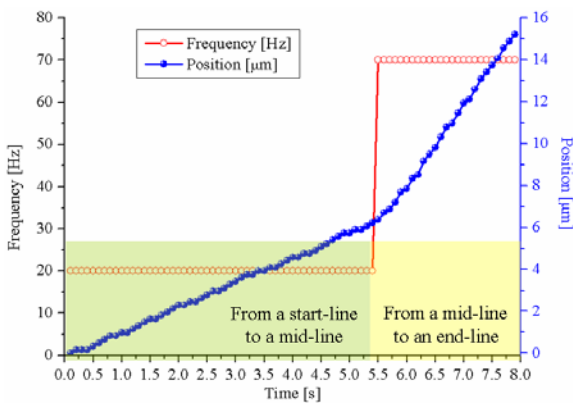


Fig.17. Experimental data of Fig.16, in case of the direct change of speed.

5 Conclusion

We proposed and described in this paper an analysis methodology for the NPA using a 3D FEM combined with an analytic method shedding light on the complex working mechanism and taking all effective components into consideration for the exact and effective characteristic analysis of the NPA and similar machines.

For the verification of this research, the mechanical system and the electrical control system of an NPA have been prototyped for a specimen manipulator.

Finally, the effectiveness of an NPA in the aspects of size, cost, and so on, the reasonableness of a clarified complex working mechanism taking all effective components into consideration, and the adequacy of the proposed analysis method have been validated by comparing these outcomes with experimental data. Also, the possibility of an NPA for a specimen manipulator is validated by experiment.

To summarize, the significant research results are as follows. The NPA has been verified as an effective precise positioning actuator in the aspects of size, cost, and so on. The possibility of the NPA for a use for a specimen manipulator has been validated by experiment. The three contact mechanism of an NPA is proposed and it is verified that this mechanism reduces the manufacturing cost and guarantees the mechanical stability of the NPA. It is also noteworthy that we have clearly clarified the complex working mechanism, the impact and inchworm, by taking all effective components into consideration. Therefore the exact and effective characteristic analysis and design of an NPA and similar machines is now possible.

References:

- [1]K. Uchino, and Jayne R. Giniwicz, "Micromechanics," Marcel Dekker, Inc. New York/Basel, 2002, ch.6.
- [2]K. Uchino, "Piezoelectric Actuator and Ultrasonic Motrs," Kluwer Academic Publishers, 1997.
- [3]Uchino, K, "Recent trend of piezoelectric actuator developments," [Micromechanics and Human Science, Proceedings of Mircromechanics and Human Science 1999 International Symposium](#), pp,3-9, 23-26 Nov. 1999.
- [4]Uchino, K, "Piezoelectric actuators/ultrasonic motors-their developments and markets," *Proceedings of the Ninth IEEE International Symposium on Applications of Ferroelectrics*, pp.319-324, 7-10 Aug. 1994
- [5]Koc B., Cagatay, S., Uchino, K., "A piezoelectric motor using two orthogonal bending modes of a hollow cylinder Ultrasonics," *IEEE Transactions on Ferroelectrics and Frequency Control*, Vol.49, pp.495 - 500, 4 Apr. 2002.
- [6]Toshiiku Sashida and Takashi Kenjo, "An Introduction to Ultrasonic Motors," Clarendon Press, Oxford, 1993.
- [7]S. Ueha, Y. Tomikawa, M. Kurosawa, and N. Nakamura, "Ultrasonic Motors: Theory and

- Applications,” Clarendon Press. Oxford, 1993, ch. 5.
- [8]Koji Ikuta, Satoshi Aritomi, and Takefumi Kabashima, “Tiny Silent Linear Cybernetic Actuator Driven by Piezoelectric Device with Electromagnetic Clamp,” *Micro Electro Mechanical Systems*, 1992, MEMS '92, Proceedings. 'An Investigation of Micro Structures, Sensors, Actuators, Machines and Robot'. IEEE.
- [9]Akihiro Torii, Haruna Kato, and Akiteru Ueda, “A Miniature Actuator with Electromagnetic Elements,” *Electrical Engineering in Japan*, Volume 134, Issue 4 , Pages 70-75.
- [10]Katsushi Furutani, Motoya Furuichi, and Naotake Mohri, “Coarse motion of `seal mechanism' with three degrees of freedom by using difference of frictional force,” *Measurement Science and Technology*, Volume 12, Issue 12, pp. 2147-2153 (2001).
- [11]H.Aoyama and A.Hayashi, “Multiple Micro Robots for Desktop Precise Production,” *Proc. Of 1st Conf. of EUSPEN*, (BREMENN) pp. 60-63, 1999.
- [12]H. Aoyama, et al, *Proc. Of 14th ASPE Annual Meeting*, (Monterey.CA), pp. 283-286, 1999.
- [13]Ohmi Fuchiwaki and Hisayuki Aoyama, “Micromanipulation by Miniature Robots in a SEM Vacuum Chamber,” *Journal of Robotics and Mechatronics*, Vol.14, No.3, 2002.
- [14]Hisayuki Aoyama and Ohmi Fuchiwaki, “Flexible Micro-Processing by Multiple Micro Robots in SEM,” *Proceedings of the 2001 IEEE International Conference on Robotics & Automation*, Seoul, Korea, May, 21-26, 2001.
- [15]Higuchi, T., Yamagata, Y., Furutani, K., Kudoh, K., “Precise Positioning Mechanism Utilizing Rapid Deformations of Piezoelectric Elements,” *IEEE transaction on Micro Electro Mechanical Systems*, pp.197-202,11-14, Feb. 1990.
- [16]Ohmichi, O., Yamagata, Y., Higuchi, T., “Micro Impact Drive Mechanisms using Optically Excited Thermal Expansion” *IEEE transaction on Microelectromechanical Systems*, Vol.6, pp.200–207, 3 Sept. 1997.
- [17]Chang-Hwan Lee, Suk-Hee Lee, Hyun-Kyo Jung, Jung-Kun Lee, and Kug-Sun Hong, “Analytic and numerical approaches for characteristic analysis of linear ultrasonic motor,” in *Electric Machines and Drives, International Conference IEMD '99*, pp. 619-621, 1999
- [18]Jong-Seok Rho, Byung-Jai Kim, Chang-Hwan Lee, Hyun-Woo Joo and Hyun-Kyo Jung, “Design and Characteristic Analysis of L1B4 Ultrasonic Motor Considering Contact Mechanism,” *IEEE Transactions on Ultrasonics, Ferroelectrics and Frequency Control*, Vol.52, pp.2054–2064, 11 Nov. 2005.
- [19]Klaus Jurgен Bathe, “Finite Element Procedures,” Prentice Hall, Inc, 1996.
- [20]Singiresu S.Rao, “Mechanical Vibrations,” 3rd ed. Addison-wesley publishing company, 1995.
- [21]Daniel J. Inman, “Engineering Vibration,” Pearson Education Korea, 2000.